Influence of Langmuir Circulation on the Deepening of the Wind-Mixed Layer

YIGN NOH AND GAHYUN GOH

Department of Atmospheric Sciences, and Global Environmental Laboratory, Yonsei University, Seoul, South Korea

SIEGFRIED RAASCH

Institute of Meteorology and Climatology, University of Hannover, Hannover, Germany

(Manuscript received 26 April 2010, in final form 21 November 2010)

ABSTRACT

Analysis of large eddy simulation data reveals that Langmuir circulation (LC) induces a significant enhancement of the mixed layer deepening, only if the mixed layer depth (MLD) h is shallow and the buoyancy jump across it ΔB is small, when simulations are initiated by applying the wind stress to a motionless mixed layer with stratification. The difference in the entrainment rate between the cases with and without LC decreases with $h\Delta B/v_L^2$, where v_L is the velocity scale of LC. The ratio of the mixing length scale l between the cases with and without LC is close to 1 for larger Rt $[=(Nl_0/q)^2; \mathrm{Rt} > \sim 1]$, but it increases to above 10 with the decrease of Rt, where N is the Brunt–Väisälä frequency and q and l_0 are the velocity and length scales of turbulence in the homogeneous layer. It is also found that, in the presence of LC, the effect of stratification on vertical mixing should be parameterized in terms of Rt instead of Ri $(=(N/S)^2)$, because velocity shear S is no longer a dominant source of turbulence. The parameterization is provided by $l/l_0 = (1 + \alpha Rt)^{-1/2}$ with $\alpha \sim 50$, regardless of the presence of LC. However, LC makes l_0 much larger than conventionally used for the boundary layer.

1. Introduction

Langmuir circulation (LC), which appears in the form of an array of alternating horizontal roll vortices with axes aligned roughly with the wind, represents one of the most important characteristics of the ocean mixed layer (see, e.g., Leibovich 1983; Smith 2001; Thorpe 2004). The prevailing theory of LC is that of Craik and Leibovich (1976), which describes the formation of LC in terms of instability brought on by the interaction of the Stokes drift with the wind-driven surface shear current. The instability is initiated by an additional ''vortex force'' term in the momentum equation as $\mathbf{u}_s \times \boldsymbol{\omega}$, where $\mathbf{u}_s$ is the Stokes drift velocity and $\boldsymbol{\omega}$ is vorticity.

Various features of LC have been reported from field observations (Weller and Price 1988; Plueddemann et al. 1996; Smith 1992, 1998; D'Asaro and Dairiki 1997; Thorpe et al. 2003; Gargett and Wells 2007). Meanwhile, recent progress in large eddy simulation (LES) has enabled us to investigate the dynamical process of LC directly (Skyllingstad and Denbo 1995; McWilliams et al. 1997; Noh et al. 2004; Min and Noh 2004; Polton and Belcher 2007; Li et al. 2005; Tejada-Martínez and Grosch 2007; Grant and Belcher 2009; Sullivan et al. 2007; Harcourt and D'Asaro 2008; Gerbi et al. 2009).

The significance of LC in the ocean mixed layer can be represented by the turbulent Langmuir number La $[=(u_*/U_s)^{1/2}]$, where u_* is the frictional velocity and U_s is the Stokes drift velocity at the surface (McWilliams et al. 1997). In particular, Li et al. (2005) and Grant and Belcher (2009) found that the transition between Langmuir turbulence and shear turbulence occurs at La $\sim$ 0.5–2. The velocity of LC v_L is shown to scale as $v_L \sim (U_s u_*^2)^{1/3}$ (Min and Noh 2004; Skyllingstad 2001; Harcourt and D'Asaro 2008; Grant and Belcher 2009), although there are observational evidences suggesting different scaling (Plueddemann et al. 1996; Smith 1998). In the presence of LC, vertical turbulent kinetic energy (TKE) is enhanced, and TKE production is dominated by the divergence of TKE flux, rather than shear production, in the mixed layer (McWilliams et al. 1997; Noh et al. 2004, 2009; Li et al. 2005; Polton and Belcher 2007; Gerbi et al. 2009).

Corresponding author address: Yign Noh, Department of Atmospheric Sciences/Global Environmental Laboratory, Yonsei University, 262 Seongsanno, Seodaemun-gu, Seoul 120-749, South Korea.
E-mail: noh@yonsei.ac.kr

DOI: 10.1175/2010JPO4494.1

It has been well established that, within the mixed layer, LC enhances vertical mixing greatly, resulting in the uniform profiles of temperature and velocity (McWilliams et al. 1997; Noh et al. 2004; Li et al. 2005; Skyllingstad 2005). Nonetheless, the question of how the mixed layer deepening is affected by the presence of LC still remains to be resolved. Evidence of enhancements to mixed layer deepening or entrainment at the mixed layer depth (MLD) in the presence of LC has been reported (Li et al. 1995; Sullivan et al. 2007; Grant and Belcher 2009; Kukulka et al. 2009). On the other hand, Weller and Price (1988) and Thorpe et al. (2003) observed no evidence that LC has a direct role in the mixed layer deepening. Skyllingstad et al. (2000) suggested from the LES results that the effects of LC are mostly confined to the initial stages of mixed layer growth.

Note that, in the presence of LC, the transport of heat and momentum can occur by means of large-scale eddies, contrary to the wall boundary layer dominated by small-scale shear-driven eddies near the wall. From this perspective, large-scale eddies associated with LC can be regarded as behaving similarly to convective eddies. However, unlike convective eddies, which are driven continuously by buoyancy force, eddies generated by LC are essentially unforced and behave inertially, because the vortex force is confined to near the surface by the decay scale of the Stokes drift. The intensity of these eddies thus decreases rapidly with depth, unlike convective eddies.

In spite of uncertainty as to the role of LC in the mixed layer deepening, there have been several attempts to incorporate its effects into the mixed layer model (Li et al. 1995; Li and Garrett 1997; D'Alessio et al. 1998; Smith 1998; McWilliams and Sullivan 2000; Smyth et al. 2002; Kantha and Clayson 2004). They considered the modification of the criterion at the MLD controlling the mixed layer deepening (Li and Garrett 1997; Smith 1998; D'Alessio et al. 1998), the inclusion of nonlocal mixing by LC (McWilliams and Sullivan 2000; Smyth et al. 2002), or the increase of TKE (D'Alessio et al. 1998; Kantha and Clayson 2004).

To evaluate and improve the mixed layer models, however, it is essential to understand properly the physical process by which LC influences the mixed layer deepening. Therefore, in the present work, we carried out LES experiments of the wind-mixed layer deepening under various conditions and analyzed the results with an aim to resolve the question on the role of LC in the mixed layer deepening and to provide information for the parameterization of its effect.

2. Simulation

The LES model used in the present simulation is similar to those used in Noh et al. (2004, 2006, 2009, 2010), Min and Noh (2004), and Noh and Nakada (2010), which have been developed based on the Parallelized LES Model (PALM) (Raasch and Schröter 2001). Langmuir circulation is realized by the Craik–Leibovich vortex force (Craik and Leibovich 1976), and wave breaking is represented by stochastic forcing. For simplicity, we assumed that both the wind stress and wave fields are in the x direction and further assumed that the wave field is steady and monochromatic. The associated Stokes velocity is then given by $u_s = U_s \exp(-4\pi z/\lambda)$ with $U_s = (2\pi a/\lambda)^2(g\lambda/2\pi)^{1/2}$, where a is the wave height, λ is the wavelength, and g is the gravitational acceleration.

Integration is initiated by applying the wind stress to a motionless fluid. The wind stress at the surface is given by $u_* = 0.02$ m s^{-1}, and no heat flux is applied at the surface. The initial MLD is set to be $h_0 = 5$ m, and the density is linearly stratified below the MLD with N^2 $(=\partial B/\partial z) = 10^{-5}, 5 \times 10^{-5}$, and 2×10^{-4} s^{-2}, which will be referred to as the case N1, N2, and N3, respectively. The buoyancy jump across the MLD ΔB is given by $N^2 h_0/2$ initially, so it can be calculated at the subsequent time automatically by $\Delta B = N^2 h/2$. Three cases of different intensity of LC are considered with $a = 0, 0.5$, and 1 m, which correspond to La $= \infty$, 0.64, and 0.32, respectively, and will be referred to as the cases L0, L1, and L2. The wavelength is fixed as $\lambda = 40$ m, but the case with $\lambda = 80$ m is also simulated for comparison. The model domain is always 300 m in the horizontal direction but 120 m (N1 and N2) or 80 m (N3) in the vertical direction. The grid size is 1.25 m in all directions. A free-slip boundary condition is applied at the bottom. The Coriolis parameter is given by $f = 10^{-4}$ s^{-1}. Quasi-equilibrium state of turbulent boundary layer is reached at about $10h_0/u_*$ ($\sim$1 h) after the onset of the wind stress. Simulations are performed for 16 h.

3. Results

a. Sensitivity of the mixed layer deepening to LC

Figure 1 compares the time series of MLD h, the buoyancy flux at the MLD $\overline{bw}(z = h)$, and $\Delta\overline{bw}(h)/\overline{bw}_0(h)$, which are obtained from the simulations with different intensity of LC (L0, L1, and L2) and different stratification below the MLD (N1 and N3). Here $\Delta\overline{bw}(h)$ represents the difference of $\overline{bw}(z = h)$ between the cases with and without LC, that is, $\Delta\overline{bw}(h) = \overline{bw}(h) - \overline{bw}_0(h)$, where $\overline{bw}_0(h)$ is the value of $\overline{bw}(h)$ in the absence of LC (La $= \infty$). Here $\overline{bw}(z = h)$ is calculated from the variation of potential energy, following Ayotte et al. (1996). The MLD is defined as the depth of the maximum N^2, as in Li and Garrett (1997). Large

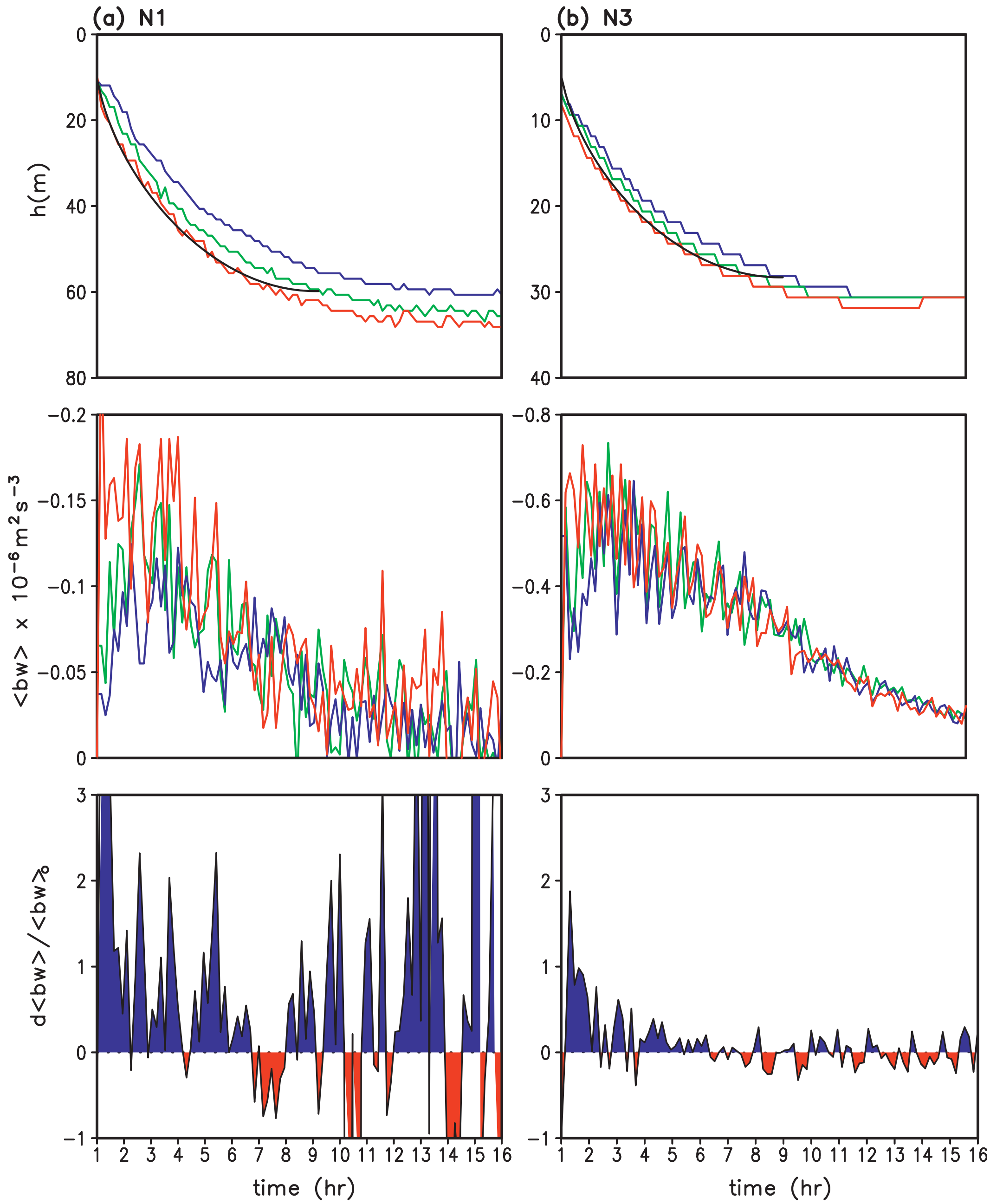

FIG. 1. Time series of (top) MLD (h), (middle) the buoyancy flux at the MLD [$\overline{bw}(z = h)$], and (bottom) $\Delta\overline{bw}(h)/\overline{bw}_0(h)$. Here, $\Delta\overline{bw}(h) = \overline{bw}(h) - \overline{bw}_0(h)$, and $\overline{bw}_0(h)$ is the buoyancy flux in the absence of LC (La = ∞). Blue is L0 (La = ∞); green is L1 (La = 0.64); red is L2 (La = 0.32); and black is the theoretical prediction by Pollard et al. (1973), which is valid only up to $t = \pi/f$: (a) N1 ($N^2 = 10^{-5}$ s^{-2}) and (b) N3 ($N^2 = 2 \times 10^{-4}$ s^{-2}).

fluctuation of $\overline{bw}(z = h)$ is due to the discontinuous increase of h over the grid size. In particular, the fluctuation of $\Delta\overline{bw}(h)/\overline{bw}_0(h)$ becomes very large in the later stage of the case N1, as $\overline{bw}_0(h)$ approaches zero.

As illustrated by Pollard et al. (1973), Niiler (1975), and Phillips (1977), the mixed layer deepening passes through two distinct stages after the onset of wind, as a result of inertial oscillation: a rapid formation and deepening of the mixed layer until half the inertial period π/f (~8.7 h) and the slow erosion thereafter. The theoretical prediction by Pollard et al. (1973) such as $h = u_*[4(1 - \cos ft)/f^2N^2]^{1/4}$, based on the assumption Ri $(=N^2/S^2) = 1$ at the MLD, is also shown in Fig. 1a, where S $\{=[(\partial U/\partial z)^2 + (\partial V/\partial z)^2]^{1/2}\}$ is velocity shear. Note that the Pollard et al.'s prediction is valid only up to $t = \pi/f$. It is interesting that a better agreement is found between LES results and the Pollard's prediction, when LC is stronger (L2). It may be related to the fact that more uniform temperature and velocity profiles are generated under stronger LC, which is consistent with the hypothesis used in Pollard's model.

Langmuir circulation is found to enhance the mixed layer deepening in general. However, the most remarkable feature in Fig. 1 is that the effect of LC, represented by $\Delta\overline{bw}(h)/\overline{bw}_0(h)$, is stronger when h is shallower in the initial stage and when stratification is weaker, as in the case N1. On the other hand, the effect of LC is negligible when stratification is strong and MLD is deep, as in the later stage of N3.

b. Variation of entrainment with LC

The factors to determine the entrainment rate w_e $(=dh/dt)$ in the presence of LC can be represented as

$$w_e = f(h, \Delta B, u_*, U_s, \lambda, f). \tag{1}$$

Dimensional analysis leads to

$$\frac{w_e}{u_*} = f\left(\frac{h\Delta B}{u_*^2}, \frac{h\Delta B}{v_L^2}, \frac{h}{\lambda}, \frac{h}{u_*/f}\right), \tag{2}$$

where v_L $[=(U_s u_*^2)^{1/3}]$ and $h\Delta B/v_L^2$ $[=(h\Delta B/u_*^2)(u_*/v_L)^2]$ are used instead of U_s and v_L/u_*. The momentum difference across MLD $[(\Delta U)^2 + (\Delta V)^2]^{1/2}$ cannot be an independent parameter, because it is determined by u_*, h, N, and f, as long as momentum is generated by wind stress.

If h/λ and $h/(u_*/f)$ remain invariant, we assume the functional form of (2) as $w_e/u_* = f_1(h\Delta B/u_*^2)[1 + f_2(h\Delta B/v_L^2)]$, where f_2 approaches zero with the increase of $h\Delta B/v_L^2$. In this case, the difference of w_e between the cases with and without LC Δw_e or equivalently $\Delta\overline{bw}(h)$ $(=\Delta w_e \Delta B)$ can be expressed as

$$\frac{\Delta\overline{bw}(h)}{\overline{bw}(h)_0} = f_2\left(\frac{h\Delta B}{v_L^2}\right). \tag{3}$$

Figure 2 clearly identifies that $\Delta\overline{bw}(h)/\overline{bw}_0(h)$ decreases with $h\Delta B/v_L^2$, which means that the effect of LC on entrainment are significant only for small h and ΔB, as observed in Fig. 1. Here data are obtained by calculating the value of $\overline{bw}(z = h)$ averaged over the period corresponding 20 m $< h <$ 30 m from each experiment to eliminate the dependence on h/λ and $h/(u_*/f)$, so the values in Fig. 2 actually represent the averaged ones over a certain range of $h\Delta B/v_L^2$, shown by horizontal bars. Note that $\Delta\overline{bw}(h)$ in Fig. 2 represents the difference of $\overline{bw}(h)$ at the same h, whereas $\Delta\overline{bw}(h)$ in Fig. 1 represents the difference of $\overline{bw}(h)$ at the same t. Figure 2 also implies that, if h and ΔB are the same, the entrainment rate increases with La^{-1} for smaller La^{-1}, but becomes insensitive to La^{-1} for larger La^{-1}, which is consistent with Fig. 16b in Grant and Belcher (2009).

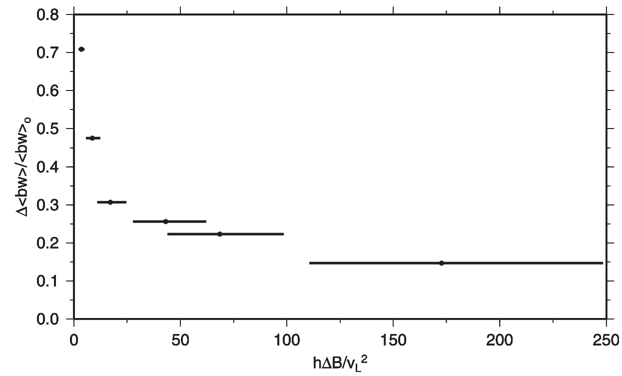

FIG. 2. Variation of $\Delta\overline{bw}(h)/\overline{bw}_0(h)$ with $h\Delta B/v_L^2$. Here data were obtained by calculating the value of $\overline{bw}(z = h)$ averaged over the period of 20 m $< h <$ 30 m from each experiment. Horizontal bars represent the corresponding range of $h\Delta B/v_L^2$.

To incorporate the effect of LC, Li et al. (1995) and Smith (1998) modified the mixed layer model by Price et al. (1986), or the PWP model, which assumes that the mixed layer deepening occurs by shear-driven turbulence when the condition

$$h\Delta B/(\Delta U)^2 < 0.65 \tag{4}$$

is satisfied at the MLD, where ΔU is the velocity jump across the MLD. In the presence of LC, they suggested that the deepening can also occur, not only when the condition (4) is satisfied but also when $h\Delta B/v_L^2$ is smaller than a critical value, or

$$h\Delta B/v_L^2 < C. \tag{5}$$

In particular, Smith (1998) suggested a critical value as $C = 9.8$ with $v_L = (U_s u_*^2)^{1/3}$. It implies that an entrained parcel must acquire kinetic energy to overcome the increase in potential energy corresponding to its being mixed over the MLD (Smith 1998).

The present result, shown in Fig. 2, is conceptually similar to the mixed layer model by Li et al. (1995) or Smith (1998), if their models are interpreted as that the mixed layer deepening by shear-driven turbulence continues until the condition in (4) is satisfied, and the additional deepening by LC occurs if the condition in (5) is satisfied. The present results imply, however, that the additional entrainment decreases gradually with

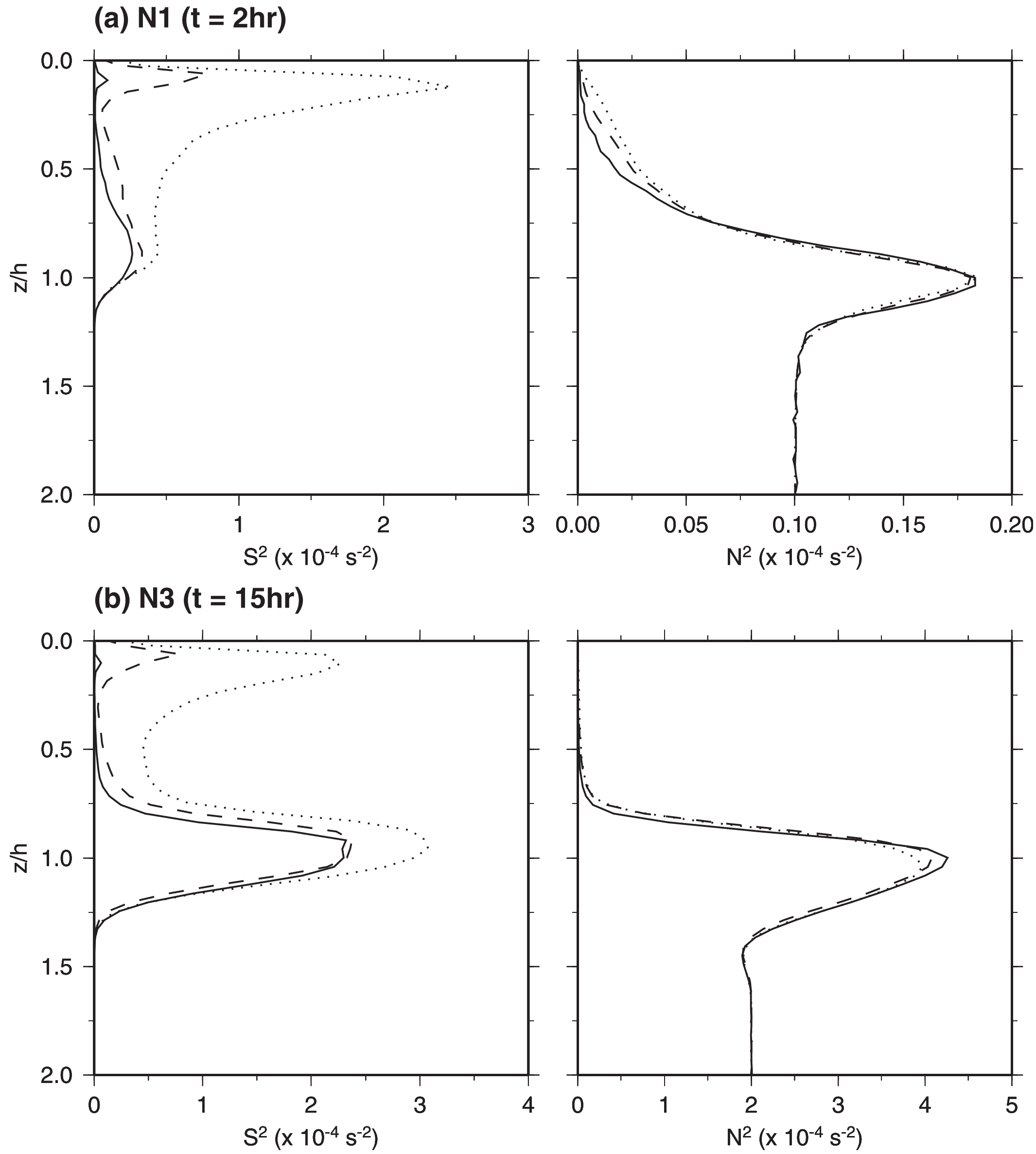

FIG. 3. Profiles of velocity shear S^2 and stratification N^2 [dotted line is L0 (La = ∞), dashed line is L1 (La = 0.64), and solid line is L2 (La = 0.32)]: (a) N1 (t = 2 h) and (b) N3 (t = 15 h).

$h\Delta B/v_L^2$ rather than disappears abruptly at a critical value of $h\Delta B/v_L^2$. The criterion $h\Delta B/v_L^2 < 9.8$, suggested by Smith (1998), roughly represents the regime of the significant effect of LC in Fig. 2.

The present result is also consistent with the previous reports that the effect of LC is mostly confined to the initial stages of mixed layer growth, and there is no evidence that LC has a direct role in mixing near the base of a 40–60-m-deep mixed layer (Weller and Price 1988; Skyllingstad et al. 2000; Thorpe 2004). The LES results (Sullivan et al. 2007; Grant and Belcher 2009; Kukulka et al. 2009), in which LC induces a noticeable increase of entrainment, were obtained under the condition in which $h\Delta B/v_L^2$ is less than 40. Note that these simulations started with the initial profiles with $\Delta T = 0°C$, h_0 larger than 30 m, and weak stratification below (e.g., $\partial T/\partial z = 0.01$ K m^{-1}).

c. *Modification of profiles in the mixed layer under LC*

Here we investigate how the profiles of various physical quantities in the mixed layer, such as velocity shear, stratification, eddy viscosity and diffusivity, and the velocity and length scales of turbulence, are modified under

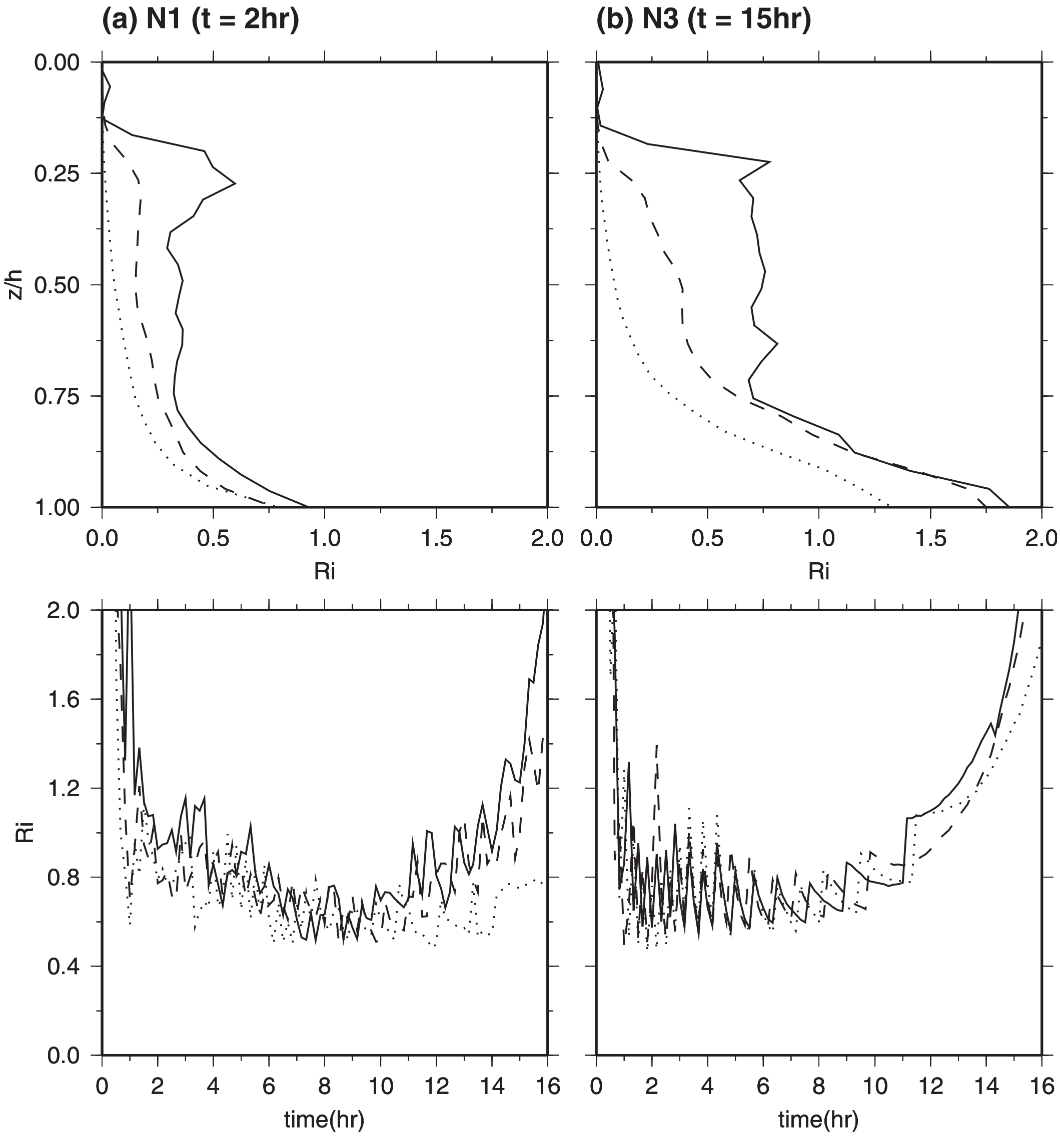

FIG. 4. (top) Profiles of Ri and (bottom) time series of Ri ($z = h$) [dotted line is L0 (La $= \infty$), dashed line is L1 (La $= 0.64$), and solid line is L2 (La $= 0.32$)]: (a) N1 ($t = 2$ h) and (b) N3 ($t = 15$ h).

the influence of LC, which helps to clarify the mechanism for the enhanced entrainment under LC. Profiles are made at $t = 2$ h for the case N1 and at $t = 15$ h for the case N3, which represent the typical cases of strong and weak effects, respectively, of LC on the mixed layer deepening, as mentioned in previous sections.

The values of S^2 are drastically decreased in the presence of LC in both cases of N1 and N3, as already reported in previous reports (McWilliams et al. 1997; Noh et al. 2004; Li et al. 2005; Skyllingstad 2005) (Fig. 3). Especially in the case of L2, S^2 almost disappears at a certain depth ($z/h \sim 0.2$), suggesting that momentum transport may occur by means of nonlocal mixing (McWilliams and Sullivan 2000; Smyth et al. 2002). Furthermore, Fig. 3 shows that S^2 decreases at the MLD as well as within the mixed layer. It should be mentioned, however, that the magnitude of shear production at the MLD is nearly the same, regardless of LC (not shown). The values of N^2 also decrease in the presence of LC, especially in the case of N1, but they are not so sensitive to the presence of LC as S^2. Generally speaking, LC always enhances vertical mixing greatly within the mixed layer, regardless of whether the contribution of LC to the mixed layer deepening is significant.

As expected from the fact that LC is more effective to reduce S^2 than N^2, Ri ($=N^2/S^2$) becomes larger under LC within the mixed layer (Fig. 4). It is also found that the decrease of Ri is less sensitive near the MLD than

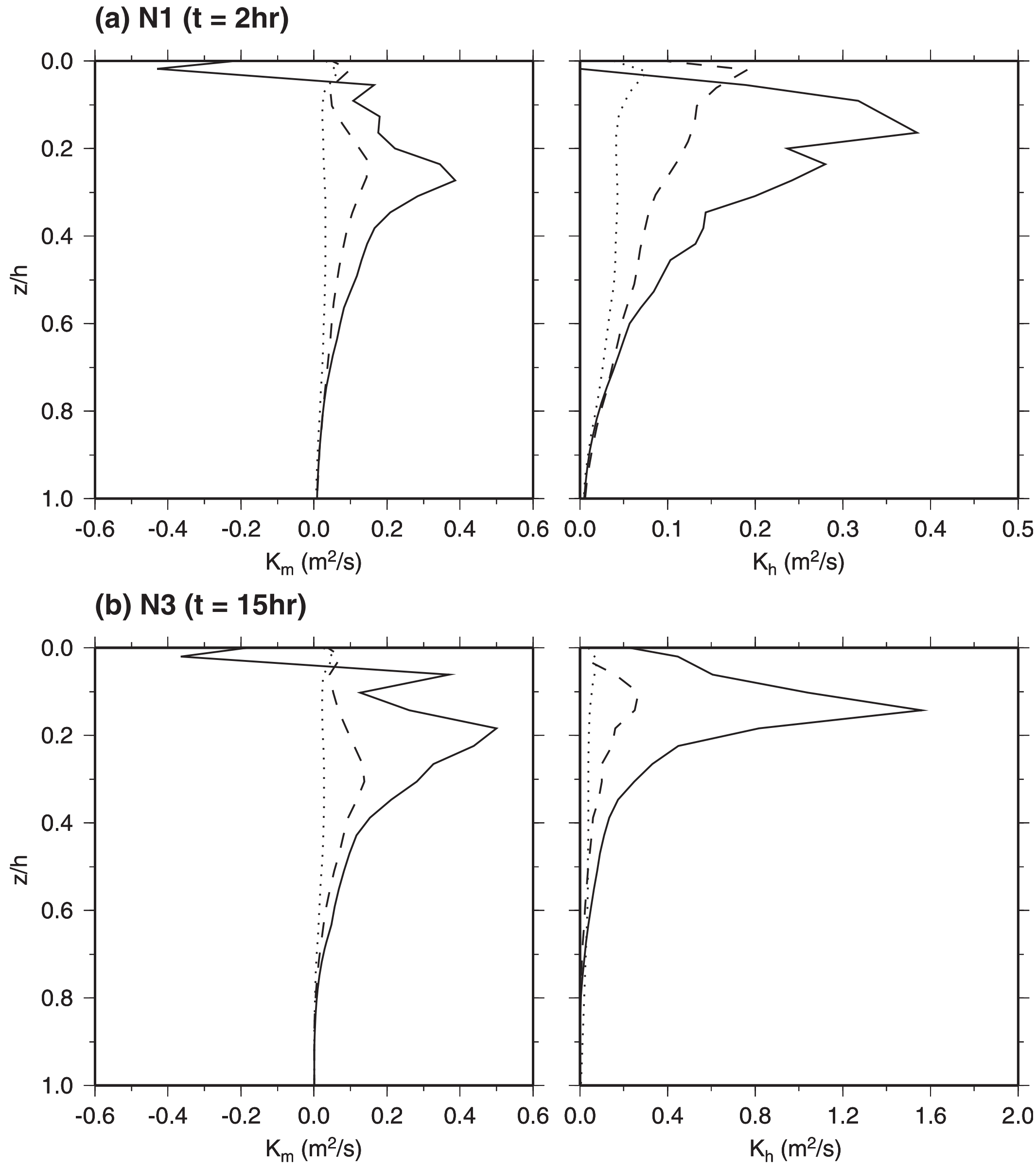

FIG. 5. Profiles of eddy viscosity K_m and eddy diffusivity K_h [dotted line is L0 (La = ∞), dashed line is L1 (La = 0.64), and solid line is L2 (La = 0.32)]: (a) N1 (t = 2 h) and (b) N3 (t = 15 h).

within the mixed layer. The time series of Ri ($z = h$) shows that Ri maintains a constant value at the MLD up to $t \sim \pi/f$ after the initial stage: that is, Ri ($z = h$) $\sim$ 0.8, which is consistent with the assumption made in Pollard et al. (1973) [Ri ($z = h$) = 1]. After the inertial period ($t > \pi/f$), however, it increases exponentially with time, as the mean velocity within the mixed layer decreases a result of inertial oscillation, as shown by Noh et al. (2010).

It is possible to consider that the increased entrainment under LC is attributed to the enhanced shear at the MLD resulting from the stronger mixing of momentum by LC within the mixed layer, as mentioned in Thorpe (2004). The decrease of S^2 ($z = h$) in the presence of LC suggests, however, that it is more likely to be attributed to the direct effect of engulfment by large-scale eddies of LC impinging on the MLD, similarly to the case of convective eddies.

In accordance with the enhanced vertical mixing within the mixed layer, much larger eddy viscosity and diffusivity, K_m and K_h, are found in the presence of LC, in both N1 and N3 (Fig. 5). Here K_m and K_h are calculated by $-\overline{uw}\partial U/\partial z - \overline{vw}\partial V/\partial z = K_m[(\partial U/\partial z)^2 + (\partial V/\partial z)^2]$ and $-\overline{bw} = K_h \partial B/\partial z$. Note that negative K_m

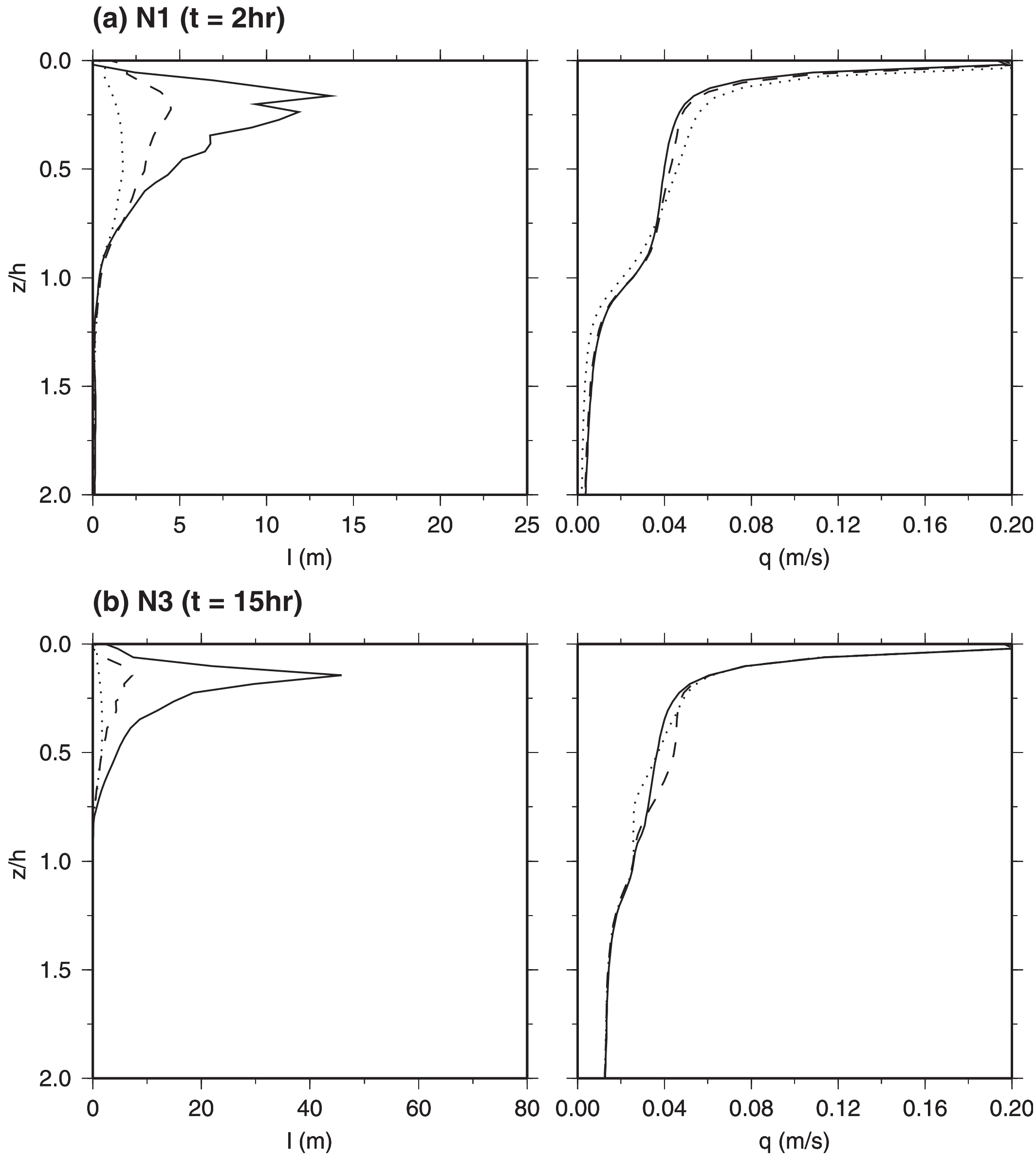

FIG. 6. Profiles of the mixing length scale l and the turbulent velocity scale q. Here, l was calculated from $K_h = S_h q l$ with $S_h = 0.49$ [dotted line is L0 (La = ∞), dashed line is L1 (La = 0.64), and solid line is L2 (La = 0.32)]: (a) N1 (t = 2 h) and (b) N3 (t = 15 h).

appears near the surface at L2, as observed by Sullivan et al. (2007), reflecting the nonlocal nature of vertical mixing by LC.

The profiles of velocity and length scales of turbulence, q [$=(\overline{u_i u_i})^{1/2}$] and l, indicate that the increase of K_m and K_h under LC is attributed predominantly to the increase of l, although both q and l increase under LC (Fig. 6). Here, l is calculated from $K_h = S_h q l$ with S_h = 0.49 (Mellor and Yamada 1982; Noh and Kim 1999). It indicates that the increase of TKE itself is not sufficient to explain the stronger vertical mixing under LC. It is also interesting to find that the ratio of l between the cases with and without LC is much larger than 1 when N^2 is small, such as at $z/h \sim 0.2$, but it is close to 1 when N^2 becomes large, such as at $z/h \sim 0.8$. This will be discussed further in the next section.

d. Parameterization of vertical mixing in the presence of LC

The suppression of vertical mixing under stratification is often parameterized in terms of Ri ($=N^2/S^2$) in mixed layer models (Pacanowski and Philander 1981; Mellor

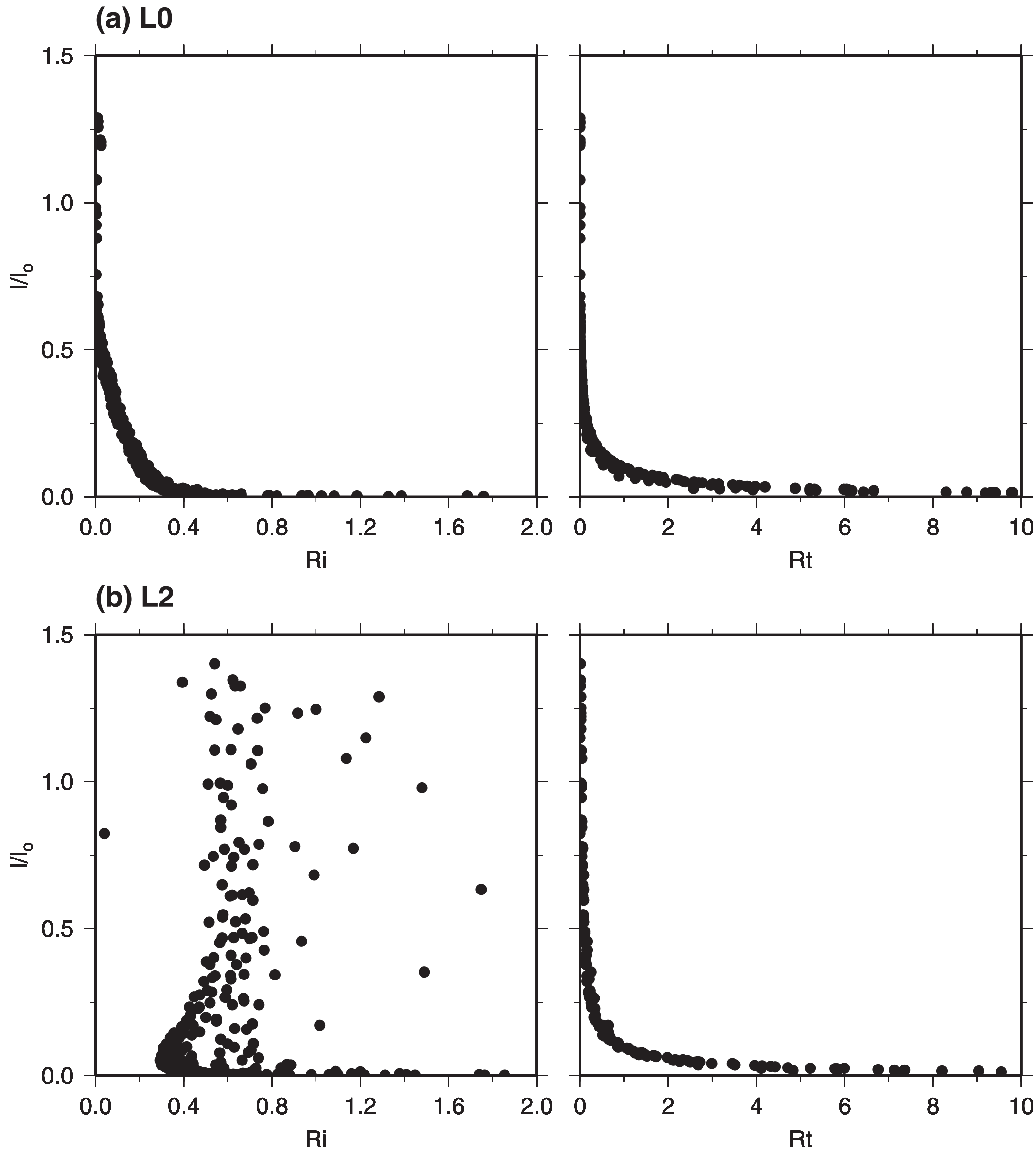

FIG. 7. Scatterplots l/l_0 vs (left) Ri and (right) Rt (N3). Data were obtained every hour at each grid depth for $z < h$ from K_h: (a) L0 and (b) L2.

and Yamada 1982; Kantha and Clayson 1994; Canuto et al. 2001). It implies that, as in the case of the atmospheric boundary layer, entrainment is dominantly contributed by turbulent eddies generated by velocity shear. This type of parameterization is usually evaluated based on the assumption of local equilibrium $P_s + P_b = \varepsilon$ with the neglect of TKE flux, where P_s is shear production, P_b is buoyancy production/decay, and ε is dissipation rate (Mellor and Yamada 1982; Kantha and Clayson 1994; Canuto et al. 2001). It has been found, however, that the divergence of TKE flux becomes a dominant turbulence source in the presence of LC (Noh et al. 2004; Sullivan et al. 2007; Polton and Belcher 2007; Grant and Belcher 2009).

Noh and Kim (1999) suggested that the parameterization of stratification on vertical mixing in the ocean mixed layer should be parameterized in terms of the Richardson number based on TKE itself {i.e., Rt [$=(Nl_0/q)^2$], rather than Ri}, because shear production is no longer a dominant source of TKE. Here, l_0 is the length scale in the homogeneous mixed layer. In particular, they suggested a formula such as

$$l/l_0 = (1 + \alpha \mathrm{Rt})^{-1/2} \tag{6}$$

with an empirical constant α, based on the assumption that l approaches the buoyancy length scale l_b ($=q/N$) with increasing stratification. Here, the length scale l_0 is prescribed by an empirical formula as

$$\frac{1}{l_0} = \frac{1}{\kappa(z+z_0)} + \frac{1}{h}, \tag{7}$$

where κ is the von Kármán constant (=0.4) and the length scale at the sea surface is given by $z_0 = 1$ m (Noh and Kim 1999). The mixed layer model based on this parameterization is shown to reproduce well the realistic upper-ocean structure (Noh and Kim 1999; Noh et al. 2002, 2005, 2007; Hasumi and Emori 2004; Rascle and Ardhuin 2009).

Figure 7 examines how l/l_0 varies with Ri and Rt for the case of N3 with and without LC (L2-N3 and L0-N3). The data were obtained every hour at each grid depth from the surface to MLD. The data l/l_0 versus Ri show a good collapse in the absence of LC, but they show a large scatter without apparent correlation in the presence of LC. It indicates that Ri is an appropriate parameter only in the case where shear production is a dominant source of TKE as in the atmospheric boundary layer. On the other hand, the data l/l_0 versus Rt show a good collapse in both cases with and without LC. Moreover, the functional forms of correlation are similar to each other, suggesting the universality of the parameterization in terms of Rt. Figure 7 convinces us that vertical mixing should be parameterized in terms of Rt instead of Ri in the ocean mixed layer.

To clarify further the relationship between l/l_0 and Rt, we plot the data from six experiments (L0-N1, L1-N1, L2-N1, L0-N3, L1-N3, and L2-N3) in the logarithmic scale for both K_m and K_h (Fig. 8). To calculate l/l_0 for K_m, $K_m = S_m ql$ is used with $S_m = 0.39$ (Mellor and Yamada 1982; Noh and Kim 1999), and the data with negative l/l_0, originating from the negative K_m near the surface in the case L2 (Fig. 4), are not included. The general pattern is similar for K_m and K_h, although data are slightly more scattered for K_m.

It is remarkable to find that the data l/l_0 versus Rt more or less collapse at larger Rt (Rt > ~1), regardless of the presence of LC, as the similarity in the relationship between l/l_0 and Rt in Fig. 7 suggests. In particular, the relationship between l/l_0 and Rt is found to follow (6) with $\alpha \sim 50$, as shown by a solid line. The slope corresponding to $l/l_0 \propto \mathrm{Rt}^{-1/2}$ indicates that l approaches $\alpha^{-1/2} l_b$ with increasing Rt.

Meanwhile, Fig. 8 also shows that, at smaller Rt (Rt < ~1), l/l_0 becomes larger in the case with LC than without LC, and the ratio of l/l_0 between the cases with and without LC continues to increase to above 10 with the

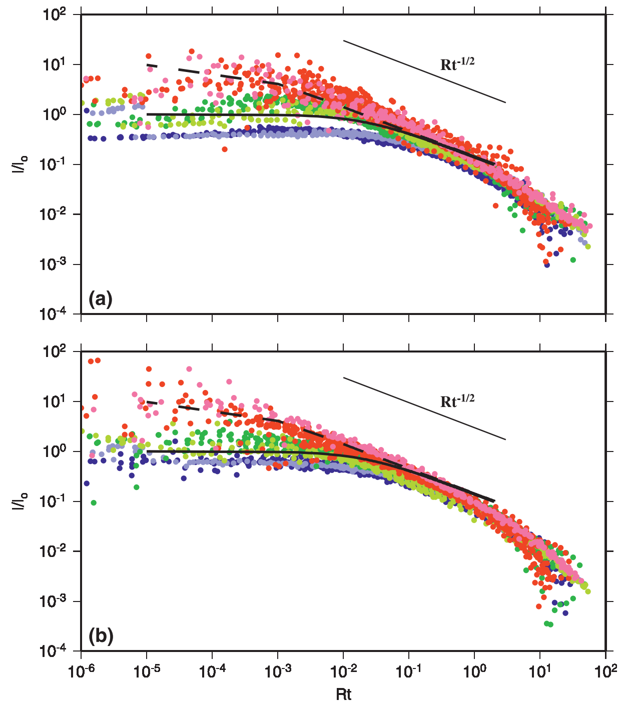

FIG. 8. Scatterplots in the logarithmic scale for l/l_0 vs Rt. Data were obtained every hour at each grid depth for $z < h$ [blue (N1, L0), light blue (N3, L0), green (N1, L1), light green (N3, L1), red (N1, L2), and light red (N3, L2)]. The black solid and dashed lines represent the predictions from $l/l_0 = (1 + \alpha\mathrm{Rt})^{-1/2}$ and $l/l_0 = \gamma(1 + \alpha\gamma^2\mathrm{Rt})^{-1/2}$, where $\alpha = 50$ and $\gamma = 10$: (a) K_m and (b) K_h.

decrease of Rt. The ratio is larger for stronger LC. Note also that l increases by more than 10 times in the presence of LC, when N^2 almost disappears at $z \sim 0.2h$, but it is less affected by LC, when N^2 becomes larger at $z \sim 0.8h$ in Fig. 6. This confirms again the fact that the influence of LC on the mixed layer deepening is important only for weaker stratification and shallower depth, as already found in Figs. 1 and 2.

The general pattern for l/l_0 versus Rt, shown in Fig. 8, can be explained in terms of the increase of l_0 under LC. Equation (6) predicts that l approaches l_0, as Rt approaches 0, whereas it approaches $\alpha^{-1/2} l_b$ independent of l_0, as Rt becomes large. Because the length scale in the presence of LC is much larger than the one given by (7), l/l_0 becomes much larger than 1 in Fig. 8 as Rt approaches 0. Consequently, we expect that the parameterization (6) remains valid, regardless of the presence of LC, but a much larger value of l_0 should be used in the presence of LC. For example, if l_0 is replaced by γl_0, (6) is modified to

$$l/l_0 = \gamma(1 + \alpha\gamma^2\mathrm{Rt})^{-1/2}. \tag{8}$$

The prediction from (8) with $\gamma = 10$ is shown to predict well the relationship between l/l_0 and Rt for the case L2

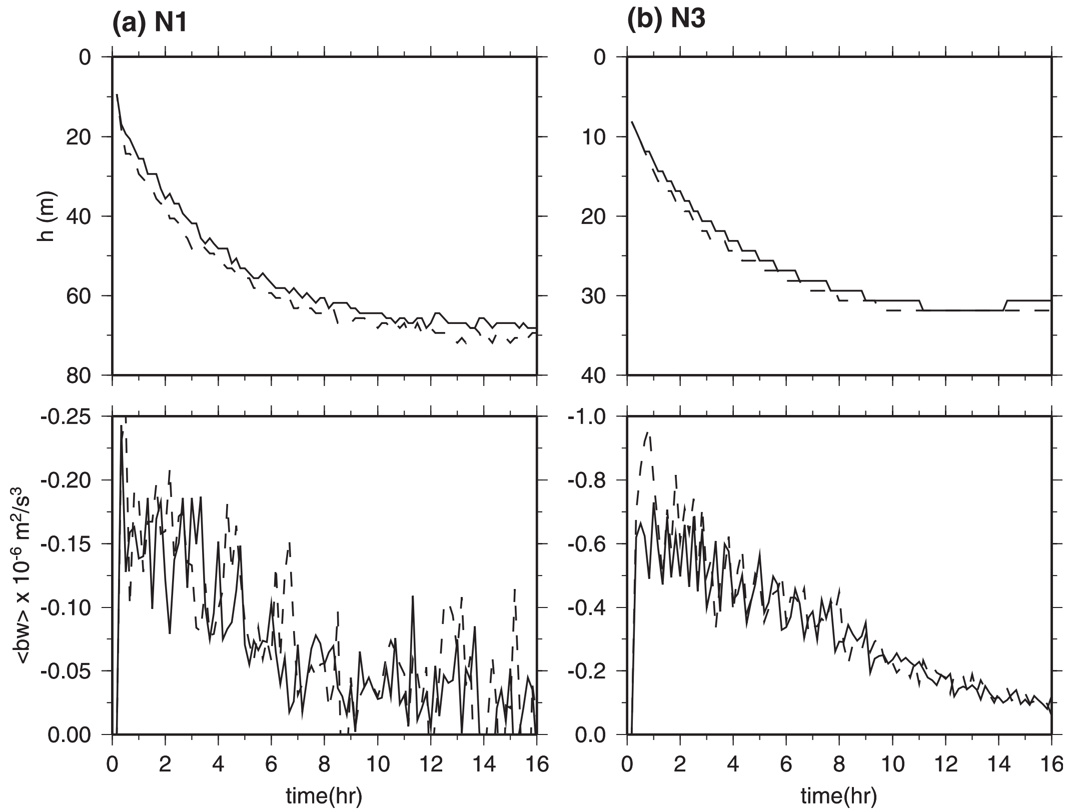

FIG. 9. Time series of (top) MLD (h) and (bottom) the buoyancy flux at the MLD [$\overline{bw}(z = h)$] for the case L2 (solid line is $\lambda = 40$ m and dashed line is $\lambda = 80$ m): (a) N1 and (b) N3.

(Fig. 7). The length scale in the presence of LC may depend on λ and h as well as La, however.

e. *Sensitivity to the e-folding depth of the Stokes drift*

It has been reported from the recent LES works that the vertical TKE can be affected by the *e*-folding depth of the Stokes drift, or λ, when λ/h is large (Harcourt and D'Asaro 2008; Grant and Belcher 2009). To investigate the sensitivity of λ to the mixed layer deepening, we compared the results with $\lambda = 40$ and 80 m for the case L2. Figure 9 shows that the effect of λ is insignificant in both N1 and N3, although the mixed layer deepening is slightly faster for larger λ in the initial stage.

4. Conclusions

Analysis of LES data reveals the consistent pattern with regard to the influence of LC on the mixed layer deepening in the present paper. That is, LC induces a significant enhancement of the mixed layer deepening only if h and ΔB are small. This property is attested by the facts that the difference of the entrainment at the MLD between the cases with and without LC decreases with $h\Delta B/v_L^2$ (Fig. 2) and that the ratio of the mixing length scale l between the cases with and without LC is close to 1 for larger Rt (Rt $> \sim 1$) but continues to increase to above 10 with the decrease of Rt (Fig. 8). The present result is in agreement with previous reports that the effect of LC is mostly confined to the initial stage of mixed layer growth (Weller and Price 1988; Skyllingstad et al. 2000; Thorpe 2004). It is also conceptually similar to the model suggested by Li et al. (1995) and Smith (2001) that the additional deepening of the mixed layer occurs in the presence of LC, when $h\Delta B/v_L^2$ becomes less than a critical value.

The magnitude of velocity shear at the MLD tends to be slightly decreased in the presence of LC (Fig. 3). It suggests that the engulfment by large-scale eddies of LC impinging on the density interface at the MLD may contribute to the increased entrainment directly, similarly to convective eddies, rather than the increased shear at the MLD. However, unlike convective eddies, which is driven continuously by buoyancy force, eddies generated by LC are essentially unforced and behave inertially, because the vortex force is confined to near the surface. Therefore, it is expected that eddies generated by LC are efficient for the vertical mixing under weak stratification, such as within the mixed layer or across the MLD with small ΔB, but their contribution to the vertical mixing becomes negligible under strong stratification, such as across the MLD with large ΔB. Moreover, the effect of LC decreases with depth, because the intensity of eddies generated by LC decreases rapidly with depth, unlike convective eddies.

Furthermore, it is clearly illustrated that the effect of stratification on vertical mixing in the presence of LC should be parameterized in terms of Rt $[=(Nl_0/q)^2]$ instead of Ri $[=(N/S)^2]$, because shear production is not a dominant source of TKE any more. In particular, the mixing length scale is parameterized by $l/l_0 = (1 + \alpha \mathrm{Rt})^{-1/2}$ with $\alpha \sim 50$, as suggested by Noh and Kim (1999), regardless of the presence of LC. However, the presence of LC makes l_0 much larger than conventionally used for the boundary layer. The inclusion of nonlocal mixing may be necessary for the more elaborate parameterization of vertical mixing, especially to account for negative K_m near the surface at small La (Fig. 5), but the present result suggests that the effect of LC can be largely represented by the increase of the mixing length scale. It is also found that the increase of K_m and K_h under LC is attributed predominantly to the increase of l, although both q and l increase under LC.

Finally, it is important to mention that the present simulation is initiated by applying the wind stress to a motionless mixed layer with stratification, which is more relevant to storm events. However, most analyses are performed after quasi-equilibrium state is reached at about $10h_0/u_*$ (~1 h) after the onset of the wind stress, which implies that the present result can be applied more generally.

Acknowledgments. This work was supported by the National Research Foundation of Korea Grant funded by the Korean Government (MEST) (NRF-2009-C1AAA001-0093068), by the Korean Ocean Research and Development Institute (KORDI) research program PE98512, and by the project ''Research for the Meteorological Observation Technology and Its Application'' at the National Institute of Meteorological Research.

REFERENCES

Ayotte, K. W., and Coauthors, 1996: An evaluation of neutral and convective planetary boundary-layer parameterizations relative to large eddy simulations. *Bound.-Layer Meteor.,* **79,** 131–175.

Canuto, V. M., A. Howard, Y. Cheng, and M. S. Dubovikov, 2001: Ocean turbulence. Part I: One-point closure model—Momentum and heat vertical diffusivities. *J. Phys. Oceanogr.,* **31,** 1413–1426.

Craik, A. D. D., and S. Leibovich, 1976: A rational model for Langmuir circulations. *J. Fluid Mech.,* **73,** 401–426.

D'Alessio, J. S. D., K. Abdella, and N. A. McFarlane, 1998: A new second-order turbulence closure scheme for modeling the ocean mixed layer. *J. Phys. Oceanogr.,* **28,** 1624–1641.

D'Asaro, E. A., and G. T. Dairiki, 1997: Turbulence intensity measurements in a wind-driven mixed layer. *J. Phys. Oceanogr.,* **27,** 2009–2022.

Gargett, A. E., and J. R. Wells, 2007: Langmuir turbulence in shallow water. Part 1. Observations. *J. Fluid Mech.,* **576,** 27–61.

Gerbi, G. P., J. H. Trowbridge, E. A. Terray, A. J. Pleuddemann, and T. Kukulka, 2009: Observation of turbulence in the ocean surface boundary layer: Energetics and transport. *J. Phys. Oceanogr.,* **39,** 1077–1096.

Grant, A. L. M., and S. E. Belcher, 2009: Characteristics of Langmuir turbulence in the ocean mixed layer. *J. Phys. Oceanogr.,* **39,** 1871–1887.

Harcourt, R. R., and E. A. D'Asaro, 2008: Large-eddy simulation of Langmuir turbulence in pure wind seas. *J. Phys. Oceanogr.,* **38,** 1542–1562.

Hasumi, H., and S. Emori, 2004: Coupled GCM (MIROC) description. K-1 Tech. Rep. 1, 39 pp.

Kantha, L. H., and C. A. Clayson, 1994: An improved mixed layer model for geophysical applications. *J. Geophys. Res.,* **99,** 25 235–25 266.

——, and ——, 2004: On the effect of surface gravity waves on mixing in the ocean mixed layer. *Ocean Modell.,* **6,** 101–124.

Kukulka, T., A. J. Plueddemann, J. H. Trowbridge, and P. P. Sullivan, 2009: Significance of Langmuir circulation in upper mixing: Comparison of observations and simulations. *Geophys. Res. Lett.,* **36,** L10603, doi:10.1029/2009GL037620.

Leibovich, S., 1983: The form and dynamics of Langmuir circulation. *Annu. Rev. Fluid Mech.,* **15,** 391–427.

Li, M., and C. Garrett, 1997: Mixed layer deepening due to Langmuir circulation. *J. Phys. Oceanogr.,* **27,** 121–132.

——, K. Zahariev, and C. Garrett, 1995: Role of Langmuir circulation in the deepening of the ocean surface mixed layer. *Science,* **270,** 1955–1957.

——, C. Garrett, and E. Skyllingstad, 2005: A regime diagram for classifying large eddies in the upper ocean. *Deep-Sea Res. I,* **52,** 259–278.

McWilliams, J. C., and P. P. Sullivan, 2000: Vertical mixing by Langmuir circulation. *Spill Sci. Technol. Bull.,* **6,** 225–237.

——, ——, and C. H. Moeng, 1997: Langmuir turbulence in the ocean. *J. Fluid Mech.,* **334,** 1–30.

Mellor, G. L., and T. Yamada, 1982: Development of a turbulent closure model for geophysical fluid problems. *Rev. Geophys. Space Phys.,* **20,** 851–875.

Min, H. S., and Y. Noh, 2004: Influence of the surface heating on Langmuir circulation. *J. Phys. Oceanogr.,* **34,** 2630–2641.

Niiler, P. P., 1975: Deepening of the wind-mixed layer. *J. Mar. Res.,* **33,** 405–422.

Noh, Y., and H. J. Kim, 1999: Simulations of temperature and turbulence structure of the oceanic boundary layer with the improved near-surface process. *J. Geophys. Res.,* **104,** 15 621–15 634.

——, and S. Nakada, 2010: Examination of the particle flux from the convective mixed layer by large eddy simulation. *J. Geophys. Res.,* **115,** C05007, doi:10.1029/2009JC005669.

——, C. J. Jang, T. Yamagata, P. C. Chu, and C. H. Kim, 2002: Simulation of more realistic upper ocean process from an OGCM with a new ocean mixed layer model. *J. Phys. Oceanogr.,* **32,** 1284–1307.

——, H. S. Min, and S. Raasch, 2004: Large eddy simulation of the ocean mixed layer: The effects of wave breaking and Langmuir circulation. *J. Phys. Oceanogr.,* **34,** 720–735.

——, Y. J. Kang, T. Matsuura, and S. Iizuka, 2005: Effect of the Prandtl number in the parameterization of vertical mixing in an OGCM of the tropical Pacific. *Geophys. Res. Lett.,* **32,** L23609, doi:10.1029/2005GL024540.

——, I. S. Kang, M. Herold, and S. Raasch, 2006: Large eddy simulation of particle settling in the ocean mixed layer. *Phys. Fluids,* **18,** 085109, doi:10.1063/1.2337098.

——, B. Y. Yim, S. H. You, J. H. Yoon, and B. Qiu, 2007: Seasonal variation of eddy kinetic energy of the North Pacific Subtropical Countercurrent simulated by an eddy-resolving OGCM. *Geophys. Res. Lett.,* **34,** L07601, doi:10.1029/2006GL029130.

——, G. Goh, S. Raasch, and M. Gryschka, 2009: Formation of a diurnal thermocline in the ocean mixed layer simulated by LES. *J. Phys. Oceanogr.,* **39,** 1244–1257.

——, ——, and ——, 2010: Examination of the mixed layer deepening process during convection using LES. *J. Phys. Oceanogr.,* **40,** 2189–2195.

Pacanowski, R. C., and S. G. H. Philander, 1981: Parameterization of vertical mixing in numerical models. *J. Phys. Oceanogr.,* **11,** 1443–1451.

Phillips, O. M., 1977: *The Dynamics of the Upper Ocean*. Cambridge University Press, 295–308.

Plueddemann, A., J. A. Smith, D. M. Farmer, R. A. Weller, W. R. Crawford, R. Pinkel, S. Vagle, and A. Gnanadesikan, 1996: Structure and variability of Langmuir circulation during the Surface Waves Processes Program. *J. Geophys. Res.,* **101,** 3525–3543.

Pollard, R. T., P. B. Rhines, and R. O. R. Y. Thompson, 1973: The deepening of the wind-mixed layer. *J. Geophys. Fluid Dyn.,* **3,** 381–404.

Polton, J. A., and S. E. Belcher, 2007: Langmuir turbulence and deeply penetrating jets in an unstratified mixed layer. *J. Geophys. Res.,* **112,** C09020, doi:10.1029/2007JC004205.

Price, J. F., R. A. Weller, and R. Pinkel, 1986: Diurnal cycles of current, temperature and turbulent diffusion in a model of the equatorial upper ocean. *J. Geophys. Res.,* **91,** 8411–8427.

Raasch, S., and M. Schröter, 2001: A large eddy simulation model performing on massively parallel computers. *Meteor. Z.,* **10,** 363–372.

Rascle, N., and F. Ardhuin, 2009: Drift and mixing under the ocean surface revisited: Stratified conditions and model-data comparisons. *J. Geophys. Res.,* **114,** C02016, doi:10.1029/2007JC004466.

Skyllingstad, E. D., 2001: Scales of Langmuir circulation generated using a large-eddy simulation model. *Spill Sci. Technol. Bull.,* **6,** 239–246.

——, 2005: Langmuir circulation. *Marine Turbulence,* H. Z. Baumert, J. H. Simpson, and J. Sündermann, Eds., Cambridge University Press, 277–282.

——, and D. W. Denbo, 1995: An ocean large-eddy simulation of Langmuir circulations and convection in the surface mixed layer. *J. Geophys. Res.,* **100,** 8501–8522.

——, W. D. Smith, and G. B. Crawford, 2000: Resonant wind-driven mixing in the ocean boundary layer. *J. Phys. Oceanogr.,* **30,** 1866–1890.

Smith, J. A., 1992: Observed growth of Langmuir circulation. *J. Geophys. Res.,* **97,** 5651–5667.

——, 1998: Evolution of Langmuir circulation during a storm. *J. Geophys. Res.,* **103,** 12 649–12 668.

——, 2001: Observations and theories of Langmuir circulation: A story of mixing. *Fluid Mechanics and the Environment: Dynamical Approaches,* J. L. Lumley, Ed., Springer, 295–314.

Smyth, W. D., E. D. Skyllingstad, G. B. Crawford, and H. Wijesekera, 2002: Nonlocal fluxes and Stokes drift effects in the K-profile parameterization. *Ocean Dyn.,* **52,** 104–115.

Sullivan, P. P., J. C. McWilliams, and W. K. Melville, 2007: Surface gravity wave effects in the oceanic boundary layer: Large-eddy simulation with vortex force and stochastic breakers. *J. Fluid Mech.,* **593,** 405–452.

Tejada-Martínez, A. E., and C. E. Grosch, 2007: Langmuir turbulence in shallow water. Part 2. Lange-eddy simulation. *J. Fluid Mech.,* **576,** 63–108.

Thorpe, S. A., 2004: Langmuir circulation. *Annu. Rev. Fluid Mech.,* **36,** 55–79.

——, T. R. Osborn, J. F. E. Jackson, A. J. Hall, and R. G. Lueck, 2003: Measurements of turbulence in the upper ocean mixing layer using Autosub. *J. Phys. Oceanogr.,* **33,** 122–145.

Weller, R. A., and J. F. Price, 1988: Langmuir circulation within the oceanic mixed layer. *Deep-Sea Res.,* **35,** 711–747.